5-15-2020

Additive Modulation of DNA-DNA Interactions by Interstitial Ions

Wei Meng
Hefei University / George Washington University

Raju Timsina
George Washington University

Abby Bull
Gettysburg College

Kurt Andresen
Gettysburg College

Xiangyun Qiu
George Washington University

Recommended Citation

Meng, Wei, Raju Timsina, Abby Bull, Kurt Andresen, and Xiangyun Qiu. "Additive Modulation of DNA-DNA Interactions by Interstitial Ions." *Biophysical Journal* 118, no. 12 (June 16, 2020): 3019–25.

Additive Modulation of DNA-DNA Interactions by Interstitial Ions

Abstract

Quantitative understanding of biomolecular electrostatics, particularly involving multivalent ions and highly charged surfaces, remains lacking. Ion-modulated interactions between nucleic acids provide a model system in which electrostatics plays a dominant role. Using ordered DNA arrays neutralized by spherical cobalt3+ hexammine and Mg2+ ions, we investigate how the interstitial ions modulate DNA-DNA interactions. Using methods of ion counting, osmotic stress, and x-ray diffraction, we systematically determine thermodynamic quantities, including ion chemical potentials, ion partition, DNA osmotic pressure and force, and DNA-DNA spacing. Analyses of the multidimensional data provide quantitative insights into their interdependencies. The key finding of this study is that DNA-DNA forces are observed to linearly depend on the partition of interstitial ions, suggesting the dominant role of ion-DNA coupling. Further implications are discussed in light of physical theories of electrostatic interactions and like-charge attraction.

Keywords

DNA, ions, electrostatics, condensation, osmotic stress

Disciplines

Biochemistry, Biophysics, and Structural Biology | Biological and Chemical Physics | Biotechnology | Physics

Additive Modulation of DNA-DNA Interactions by Interstitial Ions

Wei Meng[1,2], Raju Timsina[2], Abby Bull[3], Kurt Andresen[3*], Xiangyun Qiu[2*]

[1]Key Lab of Biofabrication of Anhui Higher Education Institution Centre for Advanced Biofabrication, Hefei University, Hefei, Anhui, 230601 China
[2]Department of Physics, George Washington University, Washington DC, 20052 USA
[3]Department of Physics, Gettysburg College, Gettysburg Pennsylvania, 17325 USA
[*]Correspondence: xqiu@gwu.edu or kandrese@gettysburg.edu

Abstract

Quantitative understanding of biomolecular electrostatics, particularly involving multivalent ions and highly charged surfaces, remains lacking. Ion-modulated interactions between nucleic acids provide a model system where electrostatics plays a dominant role. Using ordered DNA arrays neutralized by spherical Cobalt^{3+} Hexammine and Mg^{2+} ions, we investigate how the interstitial ions modulate DNA-DNA interactions. Using methods of ion counting, osmotic stress, and x-ray diffraction, we systematically determine thermodynamic quantities including ion chemical potentials, ion partition, DNA osmotic pressure/force, and DNA-DNA spacing. Analyses of the multi-dimensional data provide quantitative insights into their inter-dependencies. The key finding of this study is that DNA-DNA forces are observed to linearly depend on the partition of interstitial ions, suggesting the dominant role of ion-DNA coupling. Further implications are discussed in light of physical theories of electrostatic interactions and like-charge attraction.

Statement of Significance

Precise and predictive knowledge of biomolecular electrostatics is a long-sought goal of molecular biophysics. A primary challenge stems from the ionic, aqueous physiological environment that strongly modulates electrostatic forces between biomolecules. Understanding the roles of ions and water, despite significant advances, has been impeded by the lack of direct physical measurements of ions and water in the act of modulating electrostatic interactions. Interrogating the model system of ordered DNA arrays condensed by multivalent ions, our study makes an important contribution through first combination of multiple biophysical techniques (e.g., x-ray diffraction, ion counting, osmotic stress). Thus obtained comprehensive

thermodynamic data provide new key physical sights into long-standing questions in biomolecular electrostatics and instruct both theoretical and experimental studies in the future.

Introduction

Charges are prevalent in major classes of biomolecules such as nucleic acids, proteins, and lipids. Precise understanding of electrostatic interactions is thus a prerequisite for predictive knowledge of biomolecular behaviors (1). Nucleic acids exemplify the rich phenomena and critical roles of electrostatics in biology, ranging from RNA folding to DNA packing in viruses and sperm to chromatin assembly. In particular, nucleic acids helices (e.g., DNA/RNA duplex or triplex), with their high charge densities and atomically defined structures, make excellent model systems for physical studies of biomolecular electrostatics in aqueous ion solutions.(2) Early physical insights have come through the mean-field Poisson-Boltzmann (PB) formulation and the concept of counterion condensation, and later refinements of PB-based models were shown to quantitatively describe nucleic acids electrostatics in monovalent salts (3). However, as cation valence increases, the mean-field ansatz begins to break down, marked by its stark failure to explain multivalent-cation-mediated attraction (MCMA) between like-charged helices (4), e.g., duplex DNA condensation by trivalent cations or higher (5) and triplex DNA by divalent cations or higher (6). While it is clear that further considerations must be made, the exact physical origin of MCMA remains unclear (4).

To explain MCMA, subsequent theoretical efforts focused on non-mean-field behaviors of multivalent cations, whose discrete nature and high valence result in strong correlations between charged surfaces and cations (i.e., ions bound near the surface) (7) and in-between cations (i.e., ion-ion correlations) (8). While one key physical insight is that strong electrostatic correlation can induce like-charge attraction, these theories often disagree on the exact mechanism, with competing models such as Wigner-lattice or 2D-gas like ions (8, 9), ion bridges (10), charge density waves (11), and tightly bound ions (12). It has also been argued that non-electrostatic ion binding in the grooves, coupled with the periodic helical structures, promotes zipper-like DNA-cation correlation and DNA-DNA attraction (13). Moreover, in observation of the retention of hydration at the free energy minimum and the universal inter-DNA force-spacing dependencies, hydration force has been proposed as the effective form of inter-DNA interactions at close spacings (14, 15). Meanwhile, computer simulations made it possible to examine the full atomic details of the biomolecule-ion-water system otherwise

difficult for analytical theories or experiments. For example, point-charge cations are shown to induce attraction via positional correlation (16) and line-charge cations likely through bridging (17). Furthermore, studies of DNA vs RNA condensation revealed the importance of helical geometry and suggested externally bound cations (i.e., not in the grooves) as the most effective for mediating attraction (18, 19). Only recently have hexagonal DNA arrays been simulated at all-atomic levels, revealing the importance of packing geometry, as well as deficiencies of force fields (20). It is worth noting that the first hydration analysis of computer simulations highlighted the substantive role of solvent restructuring and solvent energetics (21, 22). Altogether, the existence of a singular mechanism becomes increasingly unlikely, and comprehensive analyses of the multi-component system are required to unravel the interplay of steric, charge, hydration, and entropic interactions in biomolecular electrostatics.

In contrast with the increasingly detailed theoretical insights, experimental knowledge of the DNA-ion-water condensates is rather limited, especially concerning the physical nature of cations at the core of competing MCMA models. Early experiments mainly examined cation characteristics in the uncondensed phase, such as the critical bulk ion concentrations for DNA condensation (23), the spatial profile and the numbers of ions around freely dispersed DNA (24-27). But very little is known about the physical properties of the counterions in the interstitial space within the condensed DNA phase. There only exist a few studies of the interstitial cations such as the concentration of polyamines in DNA condensates (28) and the binding of mono- and di-valent cations in DNA fiber (29). We recently measured the partitions of two competing, point-like cations (Mg^{2+} and $Cobalt^{3+}$ Hexammine, or CoHex) in spontaneously condensed DNA arrays (30). Variations of ion partitions were found to solely depend on a reduced variable, $[CoHex]^2/[Mg^{2+}]^3$, which prompted the proposition of an ion binding model based on entropy alone. Nonetheless, much more is unknown about the interstitial cations, e.g., how they are spatially positioned and how they modulate DNA-DNA forces.

In this study, we aim to elucidate the relationship between the partition of interstitial ions (CoHex and Mg^{2+}) and the DNA-DNA forces they mediate, by combining *DNA force* and ion counting measurements for the first time. Specifically, using the model system of condensed DNA arrays, we first vary DNA osmotic pressure (via osmotic stress) and ion chemical potentials (via buffer equilibration), and subsequently determine DNA-DNA spacing (via x-ray diffraction) and ion partitions within the array (via ion counting by atomic emission spectroscopy). Physical models

are then used to analyze the inter-dependencies between these thermodynamic quantities to gain mechanistic insights, for example, hydration force formulism for the DNA force-spacing relationship and an entropy-based ion binding model for the ion partition-chemical potential relation. Remarkably, the DNA-DNA force exhibits a linear dependence on the composition of interstitial ions or, in other words, interstitial ions modulate DNA-DNA forces additively and independently. This lack of ion-ion cooperativity suggests a prominent role of ion-DNA coupling (e.g., in contrast with ion-ion correlation) and the importance of local DNA electrostatic fields.

Methods

Preparation of ordered DNA arrays. Double-strand DNA of genomic origin was used as a model system of random-sequence B-form DNA. Salmon testes DNA from Sigma^{TM} was dialyzed against 1 M NaCl solution followed by ethanol precipitation to remove contaminants. The DNA precipitate was dried and then suspended in 1×TE buffer (10 mM Tris 1 mM EDTA pH 7.5) at ~10 mg/ml concentration as the main stock. Chloride salts of CoHex and Mg^{2+} were prepared in low buffers of 2 mM pH 7.5 Tris to minimize competition from monovalent ions. Polyethylene glycol of 8000 Dalton (PEG8k) was used as a neutral polymeric osmolyte. Ordered DNA arrays were obtained by precipitating ~300 µg DNA with PEG8k and CoHex/Mg^{2+} salts, noting that the mixed salts were used for DNA precipitation to expedite equilibration during the subsequent osmotic pressure and ion chemical potential changes. The arrays in pellet form were then equilibrated against excess bath solutions with specific CoHex, Mg^{2+}, and PEG8k concentrations (weight/weight), so as to vary the ion chemical potentials and DNA osmotic pressure in the array. Two to three changes of the bath solution with a minimum incubation time of four weeks were done to ensure equilibrium.

Measurement of DNA-DNA spacing. X-ray diffraction (XRD) was used to measure the DNA-DNA spacing of the ordered DNA phase. Our in-house x-ray scattering instrument comprises a Copper micro-focus x-ray source (Genix 3D, Xenocs) with multilayer optics, two sets of scatterless slits (×4) for beam collimation to a size of 0.8×0.8 mm, and an online 2D image plate detector (mar345, marXperts). Each DNA pellet was loaded to our home-made sample cell together with equilibrating solution. All samples were measured at room temperature and x-ray exposure time ranged from 30 to 60 minutes. Data analyses were carried out with home-written Matlab scripts. These x-ray samples were macroscopically sized and gave isotropic scattering intensities due to random packing of ordered DNA arrays. Radial integration was performed to obtain 1D scattering curves, and statistical errors were computed from the group of pixels

integrated together for a single data point. As the salt conditions in this study spontaneously condense DNA, all samples exhibited high degrees of DNA ordering. Well-defined XRD Bragg peaks were thus measured, enabling the determination of DNA-DNA spacings within 0.1 Å precision via peak fitting.

Counting the numbers of ions and phosphates. After XRD measurement, each DNA sample was dissolved in 1.5 M NaCl buffer for atomic emission spectroscopy analysis to determine the elemental concentrations of P, Co, and Mg as established in our previous study (30). Briefly, a Perkin Elmer Optima 7300DV (Perkin Elmer, Waltham, MA) was used to measure the numbers of Co, Mg, and P (from the DNA); all measurements were made in the Axial mode. Samples were diluted to provide replicate measurements and allow for measurement in the linear regime. Six independent measurements utilizing two independent controls were averaged. Each control consisted of six linearly spaced samples that spanned the entire range of concentrations. Measurements were averaged and the standard error of the mean was calculated.

Results

Multidimensional measurements and inter-dependencies of the thermodynamic states of DNA arrays. Probing the system of DNA arrays interspersed with ions and water, our integrative approach measures the following quantities: ion chemical potential, ion partition (the relative fractions of CoHex and Mg^{2+} ions within the DNA arrays), DNA-DNA spacing, and DNA-DNA force in terms of DNA osmotic pressure. Among them, it is intuitive to consider DNA-DNA spacing and ion chemical potential as independent variables that uniquely determine the DNA-DNA force and ion partition. An illustration of such multidimensional data is given in Fig. 1, with each curve under constant ion chemical potentials of CoHex and Mg^{2+} (i.e., constant ion concentrations in the bath solution).

The DNA-DNA force-spacing curves, also referred to as the DNA osmotic equation of state, are shown in Fig. 1a with the force given as pressure. Under a constant [CoHex] of 1 mM and varied [Mg^{2+}] between 0-20 mM, DNA spontaneously condenses, resulting in finite DNA-DNA spacings at zero DNA-DNA force/pressure. DNA-DNA force rises from zero upon being pushed to closer spacings by the osmolyte PEG8k, giving a convex curve on the log-linear scale. In Mg^{2+} only solutions where DNA-DNA interaction is always repulsive, the force-spacing curve extends to infinity because zero force can only be achieved at infinite DNA-DNA spacing, as shown for 20 mM Mg^{2+} in Fig. 1a. Overall, the measured force-spacing curves exhibit the

hydration force characteristics studied in detail by Parsegian, Rau, and coworkers (14, 31). One salient feature is a dominant short-range, repulsive hydration force at the closest spacings (e.g., <26 Å), which is an exponential force with a universal decay length ~2.4 Å (14). Other force terms, necessarily of longer range, become discernable at larger spacings if present. CoHex-mediated attraction is manifested as an attractive hydration force with twice the decay length of the short-range hydration repulsion (15). Non-condensing ions typically give an additional electrostatic repulsion, while the Mg^{2+}-only force curve here shows negligible residual electrostatic repulsion beyond the short-range hydration repulsion. With hydration forces as the predominant contributions to all measured forces in this study, DNA osmotic pressure can be described by $\Pi(d) = \Pi_R e^{-d/\lambda} + \Pi_A e^{-d/2\lambda}$, where d is the DNA-DNA spacing, λ the decay length ~2.4 Å, and Π_R and Π_A the magnitudes of the hydration repulsion and attraction respectively (see Ref. 14 for details). This double-exponential form is used to fit the curves with Π_R and Π_A as fitting parameters; excellent agreements are obtained (Fig. 1a).

The partitions of interstitial ions (ions within the condensed arrays; in this work CoHex and Mg^{2+}) are shown in Fig. 1b as the charge ratios between each ion and DNA phosphate, f_{Co} ($3\times n_{Co}/n_P$) and f_{Mg} ($2\times n_{Mg}/n_P$), noting that the ion numbers here (n_{Co} and n_{Mg}) are absolute numbers of interstitial ions rather than the differences from the bulk. Therefore f_{Co} and f_{Mg} essentially give the fraction of DNA charges neutralized by each ion. As expected from charge neutrality of the macroscopic DNA array, their sum $f_{Co}+f_{Mg}$ remains unity for all samples (Fig. 1b). This also indicates the exclusion of Cl^- ions or CoHex-Cl^- ion pairs from the array, which simplifies the composition of interstitial ions for quantitative analysis. Note that our experiments aimed to minimize the effect of CoHex-Cl^- ion pairing by choosing a relatively low bath [CoHex] of 1 mM and [Mg^{2+}] between 0 and 20 mM. Mechanistically, the competition between CoHex and Mg^{2+} for the interstitial space can be rationalized in terms of electrostatics and entropy. Because of stronger CoHex-DNA electrostatic attraction than Mg^{2+}-DNA, f_{Co}/f_{Mg} ratio is much larger than the [CoHex]/[Mg^{2+}] ratio in the bath and the ratio increases with decreasing DNA-DNA spacing due to the intensifying DNA electrostatic field. At a given inter-DNA spacing, f_{Co} and f_{Mg} vary strongly with the bath [CoHex]/[Mg^{2+}], evidencing significant entropic contributions (see the model below). Consequently, the partition of interstitial CoHex and Mg^{2+} results from an equilibrium between two ion phases: the dilute bulk phase in the bath solution and the interstitial phase within the array.

A phenomenological model based on ion entropy and electrostatics to describe the dependencies of ion partitions. We next aim to explain the CoHex vs Mg^{2+} two-phase equilibrium at a phenomenological level. The ion chemical potentials in the free bulk phase are dominated by the entropies of mixing, mathematically represented as ln[CoHex] and ln[Mg^{2+}], while both ion entropies and electrostatic energies are important for the interstitial phase. As the spatial organization of interstitial ions is still unknown, we consider a simplified case of random CoHex/Mg^{2+} distribution, regardless of being continuous or site-bound. Ion entropies are then taken as ln(n_{Co}/V) and ln(n_{Mg}/V), where n_{Co} (n_{Mg}) is the number of interstitial CoHex (Mg^{2+}) ions given by $\lambda f_{Co}/3$ ($\lambda f_{Mg}/2$) with λ as the linear charge density of DNA, and the interstitial volume V for a 2D hexagonal cell of unit length is given by $\sqrt{3}d^2/2 - \pi r_0^2$ with d as the inter-axial spacing and r_0 the DNA radius of 10 Å. For ion electrostatic energies, it is difficult to estimate their absolute values without a quantitative theory of MCMA, and a fitting parameter for the electrostatic energy difference is used as described below. As in our previous study (30), we consider a virtual exchange of 2 CoHex and 3 Mg^{2+} ions between the two phases as dictated by charge neutrality. When at equilibrium, the total free energy is unchanged over this virtual exchange, resulting in the following equation,

$$3\ln(n_{Mg}/V) - 2\ln(n_{Co}/V) + \Delta E = 3\ln([Mg^{2+}]) - 2\ln([CoHex]) = \ln([Mg^{2+}]^3/[CoHex]^2) \quad (1).$$

Here ΔE (kT) includes the difference in ion electrostatic energies $\Delta E_{DNA\text{-}ion}$ caused by the ion exchange and the difference in reference-state chemical potentials ΔE_0 (e.g., due to different ion spatial organizations and entropies between the two ion phases). Though the reference state for the bath ion phase is invariant, the interstitial phase changes substantially with DNA-DNA spacing which modulates both DNA-ion interactions and ion distribution. ΔE thus strongly depends on DNA-DNA spacing. Conversely, ΔE is expected to remain constant if DNA-DNA spacing stays constant. Indeed we observe that DNA-DNA spacing is largely independent of the bath ion concentrations (see Suppl. Fig. S3) under a constant osmotic pressure. We then fit the ion partitions vs bath ion concentrations under a given osmotic pressure with ΔE as the only fitting parameter. Good agreements are obtained for all curves as shown in Fig. 2 (see Suppl. Fig. S4 for additional fits), noting that the free [CoHex] in the bath phase is corrected for the Co^{3+}Hex-Cl^- ion pairing with a binding constant of 20 mM (30). Consistent with our previous observation under zero osmotic pressure (30), the changes of ion partitions in the interstitial

space can be accounted for solely by the changes in ion entropies, provided that the DNA-DNA spacing does not change significantly.

Furthermore, as expected from the strong dependence of ΔE on DNA-DNA spacing, the fitted ΔE values increases noticeably with decreasing DNA-DNA spacing (i.e., increasing osmotic pressure), by ~2.1 kT from ~28 to ~24 Å (corresponding to an increase of [PEG8k] from 0% to 40% weight/weight). This can be attributed to stronger DNA-ion electrostatic coupling with closer DNA-DNA spacing, which favors CoHex over Mg^{2+} and yields a larger ΔE. For this reason, Equation 1 with ΔE as constant fails to describe the ion partition vs. DNA-DNA spacing relations (see Suppl. Fig. S2). A holistic analysis of the dependence of ion partition on both DNA-DNA spacing and ion chemical potentials would require a detailed model of MCMA in order to calculate ΔE. In lieu of such theoretical model, this phenomenological model is instructive in showing that ideal mixing behaviors can characterize ion entropies in the interstitial space in counter to ion-ion correlations beyond mean-field considerations. Furthermore, the variations of fitted ΔE values may provide a quantitative measure of ion-DNA coupling to guide theoretical developments.

Additive modulation of DNA-DNA forces by interstitial ions. Evident from the distinctive force-spacing curves in Fig. 1, the partition of interstitial CoHex and Mg^{2+} ions strongly modulates DNA-DNA forces. With parameterization in the form of double exponentials, each force curve is reduced to two parameters, Π_R and Π_A, the magnitudes of the short-range repulsion and medium/long-range attraction respectively. For the two asymptotic cases, the force curve with CoHex only (i.e., f_{Co}=1 with 0 mM [Mg^{2+}] in the bath) gives Π_R of 418.4 GPa and Π_A of -1.3 GPa, and the curve with Mg^{2+} only (i.e., f_{Mg}=1 with 0mM [CoHex] in the bath) gives Π_R of 201.8 GPa and Π_A of -0.3 GPa. The slightly negative Π_A for Mg^{2+} may appear unexpected, but consistent with a recent study of DNA phase transition reporting a universal medium-range attraction even in monovalent salts (32). It is worth noting that the CoHex-only curve gives larger Π_R than the Mg^{2+}-only curve, which likely originates from stronger hydration or larger size of CoHex ions enhancing short-range repulsion. The stronger repulsion and attraction with CoHex than Mg^{2+} result in an interesting crossover between the two curves at DNA-DNA spacing d~25.5 Å, i.e., an isobaric spacing independent of ion partitions which can be discerned in Fig. 1a and in Suppl. Fig. S1. In Fig. 3a, we show the force magnitudes Π_R and Π_A as functions of the bath [Mg^{2+}] (with [CoHex] at a fixed 1 mM for all), noting that each force curve

was measured under constant [CoHex] and [Mg^{2+}] in the bath. Both Π_R and Π_A change monotonically as expected and, interestingly, both appear to exhibit a linear dependence on [Mg^{2+}]. The linear dependency prompts us to examine the relation between the force magnitudes and ion partitions. Due to the variations of ion partitions along each force curve (Suppl. Fig. S2), the representative f_{Co} values (i.e., 1-f_{Mg}) at 30% PEG8k (d~26 Å) are used as the x-axis in Fig. 3b. Using f_{Co} as x-axis also makes it possible to plot results from force curves in higher [Mg^{2+}] or zero [CoHex] salts that do not condense DNA spontaneously. Fig. 3b shows that linear relations hold for both Π_R and Π_A across the full range of f_{Co}, and the linear trends are independent of the choice of representative f_{Co} values for the curve (see Suppl. Fig. S5). It should be noted that this observation is subject to the limitations of experimental uncertainties and the finite number of data points. Taken together, these observations reveal that DNA-DNA forces are linearly dependent on the partition of interstitial ions. In other words, interstitial ions modulate DNA-DNA forces additively and each ion appears to act independently of other ions. Significant ion-ion coupling in DNA-DNA attraction would result in super-linear dependence on the CoHex fraction, e.g., a convex shaped curve towards f_{Co}=1 for negative Π_A values in Fig. 3b which is noticeably absent.

Additive modulation of DNA-DNA forces by interstitial ions gives rise to an interesting outcome that, with the knowledge of any two force-spacing curves and their ion partitions, one can predict all other force-spacing curves with different ion partitions. As the experimental data were collected under the same grids of osmotic pressures, a useful test is to compare measured and predicted DNA-DNA spacings. Specifically, with the experimental values of osmotic pressure Π and ion partition f_{Co}, the predicted DNA spacing d is obtained via an iterative search to satisfy $\Pi(d,f_{Co}) = f_{Co}\times\Pi(d,f_{Co}=1)+(1-f_{Co})\times\Pi(d,f_{Co}=0)$, where $\Pi(d,f_{Co}=1)$ and $\Pi(d,f_{Co}=0)$ are the double-exponential fits of the force-spacing curves with asymptotic ion partitions (i.e., with CoHex or Mg^{2+} only). Fig. 4 shows the comparison between such predicted spacings and experimental values, noting that this prediction method allows the use of exact f_{co} value for every data point rather than the average. While good agreements are observed in short ranges d<28Å (i.e., high pressure), the predicted d-spacings appear to be slightly greater than the measurements under lower pressures. One likely cause is that the DNA array takes on salt-dependent structure phases under lower pressures (32) (see Suppl. Fig. S6 for further explanations), such as a

disordered hexagonal phase with Mg^{2+} and a more ordered hexatic phase with CoHex, which complicates the prediction under lower pressures.

Discussion

In summary, we have combined x-ray diffraction (for DNA-DNA spacing), osmotic stress (for DNA-DNA pressure), and atomic emission spectroscopy (for ion partition) to interrogate the system of ordered DNA arrays bathed in a series of CoHex and Mg^{2+} ion solutions. These multi-dimensional thermodynamic measurements, being the first to our knowledge, not only yield systematic experimental data for theoretical advancement but also provide new physical insights on biomolecular electrostatics. Measured force-spacing relations are congruent with the hydration force formulation of double exponentials, while it is noted that our subsequent analyses are not contingent on the hydration force theorem and the form of double exponentials largely serves as a way to parameterize the force curves. The variations of ion partitions with respect to the ion chemical potentials (i.e., bath ion concentrations) are described reasonably well by a phenomenological model based on ion entropies. However, this model fails to explain the dependence of ion partitions on DNA-DNA spacing, for which more sophisticated treatise of electrostatic energies would be required. Most importantly, our multi-dimensional measurements allow for the first examination of how DNA-DNA forces depend on the compositions of interstitial ions. This leads to a remarkable observation that ions mediate DNA-DNA forces additively, suggesting that ions are predominantly coupled with DNA rather than with other ions.

On the premise of dominant ion-DNA coupling, one direct consequence is that the atomic structure of DNA is expected to be an important factor in addition to the extensively studied ion valence and structure, as both the structural and electrostatic details of DNA surface necessarily modulate the distribution and dynamics of ions and consequently the interaction between DNA helices. This proposition is supported by recent studies of the role of DNA sequence and modifications in DNA-DNA interactions. For example, homopolymeric A:T duplexes give stronger inter-DNA attraction than random sequences due to stronger ion binding into the major grooves, and methylation of Cytosine would weaken the electrostatic attraction due to hampered groove binding (33). Moreover, the A-form double helix of RNA represents a significant departure from the canonical B-form helix by sequestering ions within its deep grooves and surprisingly suppressing attraction (18). Such modulations of nucleic acids interactions, albeit weak at the single base level, are quickly multiplied by the length of the

sequence, giving rise to the notion of structure-directed regulation of nucleic acids behaviors such as transcription factor binding (34). It is also conceivable that multiple repeats of a specific sequence motif at the genomic scale could develop enough multivalency to shape chromosome structure and function. Physical understanding of nucleic acids interactions at the atomic resolution is thus much needed to illuminate their functional roles.

Furthermore, the multi-component nature of the system calls for synergistic approaches integrating experiments, theories, and simulations to dissect and quantitate the contributions from DNA, ions, and solvent. In particular, all measured quantities in this study, being thermodynamic in nature, can be readily extracted from all-atom MD simulations of DNA arrays such as in Ref. 22, and detailed comparisons should be powerful for validating simulations and gaining mechanistic insights. Altogether, the results from this multi-pronged systematic study make an important step towards physical understanding of ion-modulated nucleic acids interactions, and efforts are under way to probe the role of DNA and ion structures.

Acknowledgements

This work was supported by the National Science Foundation (USA) through the MCB-1616337 award. We thank the late Donald Rau (National Institutes of Health) for valuable discussions at the early stage of this work.

Author contributions.

X.Q. designed research; W.M. and R.T. conducted osmotic stress measurements; A.B. and K.A. conducted ion counting measurements; K.A. and X.Q. analyzed data and wrote the manuscript. All authors have read and approved the manuscript.

Competing financial interests: The authors declare no competing financial interests.

Materials & Correspondences: K.A. or X.Q.

Bibliography

1. Ren, P., J. Chun, D. G. Thomas, M. J. Schnieders, M. Marucho, J. Zhang, and N. A. Baker. 2012. Biomolecular electrostatics and solvation: a computational perspective. Q. Rev. Biophys. 45:427-491.
2. Gelbart, W. M., R. F. Bruinsma, P. A. Pincus, and V. A. Parsegian. 2000. DNA-inspired electrostatics. Physics Today 53:38-44.
3. Lipfert, J., S. Doniach, R. Das, and D. Herschlag. 2014. Understanding Nucleic Acid-Ion Interactions. In Annual Review of Biochemistry, Vol 83. R. D. Kornberg, editor. Annual Reviews, Palo Alto. 813-841.

4. Teif, V. B., and K. Bohinc. 2011. Condensed DNA: condensing the concepts. Prog Biophys Mol Biol 105:208-222.
5. Li, L., S. A. Pabit, S. P. Meisburger, and L. Pollack. 2011. Double-stranded RNA resists condensation. Phys. Rev. Lett. 106:108101.
6. Qiu, X., V. A. Parsegian, and D. C. Rau. 2010. Divalent counterion-induced condensation of triple-strand DNA. Proc Natl Acad Sci U S A 107:21482-21486.
7. Naji, A., and R. R. Netz. 2004. Attraction of like-charged macroions in the strong-coupling limit. Eur Phys J E Soft Matter 13:43-59.
8. Rouzina, I., and V. A. Bloomfield. 1996. Macroion attraction due to electrostatic correlation between screening counterions .1. Mobile surface-adsorbed ions and diffuse ion cloud. J. Phys. Chem. 100:9977-9989.
9. Shklovskii, B. I. 1999. Wigner crystal model of counterion induced bundle formation of rodlike polyelectrolytes. Phys. Rev. Lett. 82:3268-3271.
10. Solis, F. J., and M. O. de la Cruz. 1999. Attractive interactions between rodlike polyelectrolytes: Polarization, crystallization, and packing. Physical Review E 60:4496-4499.
11. Angelini, T. E., H. Liang, W. Wriggers, and G. C. Wong. 2003. Like-charge attraction between polyelectrolytes induced by counterion charge density waves. Proc Natl Acad Sci U S A 100:8634-8637.
12. Tan, Z. J., and S. J. Chen. 2006. Ion-mediated nucleic acid helix-helix interactions. Biophys. J. 91:518-536.
13. Kornyshev, A. A., and S. Leikin. 1999. Electrostatic zipper motif for DNA aggregation. Phys. Rev. Lett. 82:4138-4141.
14. Stanley, C., and D. C. Rau. 2011. Evidence for water structuring forces between surfaces. Curr Opin Colloid Interface Sci 16:551-556.
15. Rau, D. C., and V. A. Parsegian. 1992. Direct Measurement of the Intermolecular Forces between Counterion-Condensed DNA Double Helices - Evidence for Long-Range Attractive Hydration Forces. Biophys. J. 61:246-259.
16. GronbechJensen, N., R. J. Mashl, R. F. Bruinsma, and W. M. Gelbart. 1997. Counterion-induced attraction between rigid polyelectrolytes. Phys. Rev. Lett. 78:2477-2480.
17. Dai, L., Y. Mu, L. Nordenskiold, and J. R. van der Maarel. 2008. Molecular dynamics simulation of multivalent-ion mediated attraction between DNA molecules. Phys. Rev. Lett. 100:118301.
18. Tolokh, I. S., S. A. Pabit, A. M. Katz, Y. Chen, A. Drozdetski, N. Baker, L. Pollack, and A. V. Onufriev. 2014. Why double-stranded RNA resists condensation. Nucleic Acids Res. 42:10823-10831.
19. Wu, Y. Y., Z. L. Zhang, J. S. Zhang, X. L. Zhu, and Z. J. Tan. 2015. Multivalent ion-mediated nucleic acid helix-helix interactions: RNA versus DNA. Nucleic Acids Res. 43:6156-6165.
20. Yoo, J., and A. Aksimentiev. 2016. The structure and intermolecular forces of DNA condensates. Nucleic Acids Res. 44:2036-2046.
21. Podgornik, R., J. Zavadlav, and M. Praprotnik. 2018. Molecular Dynamics Simulation of High Density DNA Arrays. Computation 6.
22. Zavadlav, J., R. Podgornik, and M. Praprotnik. 2017. Order and interactions in DNA arrays: Multiscale molecular dynamics simulation. Sci. Rep. 7:4775.
23. Pelta, J., F. Livolant, and J. L. Sikorav. 1996. DNA aggregation induced by polyamines and cobalthexamine. J. Biol. Chem. 271:5656-5662.

24. Pollack, L. 2011. SAXS studies of ion-nucleic acid interactions. Annu Rev Biophys 40:225-242.
25. Bai, Y., M. Greenfeld, K. J. Travers, V. B. Chu, J. Lipfert, S. Doniach, and D. Herschlag. 2007. Quantitative and comprehensive decomposition of the ion atmosphere around nucleic acids. J. Am. Chem. Soc. 129:14981-14988.
26. Jacobson, D. R., and O. A. Saleh. 2017. Counting the ions surrounding nucleic acids. Nucleic Acids Res. 45:1596-1605.
27. Pabit, S. A., S. P. Meisburger, L. Li, J. M. Blose, C. D. Jones, and L. Pollack. 2010. Counting ions around DNA with anomalous small-angle X-ray scattering. J. Am. Chem. Soc. 132:16334-16336.
28. Teif, V. B. 2005. Ligand-induced DNA condensation: choosing the model. Biophys. J. 89:2574-2587.
29. Korolev, N., A. P. Lyubartsev, A. Rupprecht, and L. Nordenskiold. 1999. Competitive binding of Mg2+, Ca2+, Na+, and K+ ions to DNA in oriented DNA fibers: experimental and Monte Carlo simulation results. Biophys. J. 77:2736-2749.
30. Qiu, X., J. Giannini, S. C. Howell, Q. Xia, F. Ke, and K. Andresen. 2013. Ion competition in condensed DNA arrays in the attractive regime. Biophys. J. 105:984-992.
31. Parsegian, V. A., and T. Zemb. 2011. Hydration forces: Observations, explanations, expectations, questions. Current Opinion in Colloid & Interface Science 16:618-624.
32. Yasar, S., R. Podgornik, J. Valle-Orero, M. R. Johnson, and V. A. Parsegian. 2014. Continuity of states between the cholesteric -> line hexatic transition and the condensation transition in DNA solutions. Sci. Rep. 4.
33. Yoo, J., H. Kim, A. Aksimentiev, and T. Ha. 2016. Direct evidence for sequence-dependent attraction between double-stranded DNA controlled by methylation. Nat Commun 7:11045.
34. Li, J. S., J. M. Sagendorf, T. P. Chiu, M. Pasi, A. Perez, and R. Rohs. 2017. Expanding the repertoire of DNA shape features for genome-scale studies of transcription factor binding. Nucleic Acids Res. 45.

Figure Captions

Fig. 1. Illustrations of DNA-DNA forces and ion partitions as functions of the DNA-DNA spacing. (a) Representative measured force-spacing dependencies are shown as symbols in bath salts of 1 mM CoHex and [Mg^{2+}]s of 0 (□), 5(○), 10(▷), and 20 (◊) mM, as well as in 0 mM CoHex 20 mM Mg^{2+} (△). Each corresponding curve fit with the double-exponential hydration force formalism is plotted as a solid line of the same color, and the difference between the data and fit is given in the same symbol with an offset below. (b) Representative measured ion partitions as functions of DNA-DNA spacing are shown as symbols linked by lines as guide to the eye. The same symbol is used for the three values (f_{Co}, f_{Mg}, and f_{Co}+f_{Mg}) under each bath ion condition: 1 mM CoHex and [Mg^{2+}]s of 2 (□), 7 (○), and 17 (▷) mM. The different trends exhibited by the three values aid their distinction: f_{Co} decreases, f_{Mg} increases, and f_{Co}+f_{Mg} is largely constant ~1. Data below a DNA-DNA spacing of 24.5 Å are discarded because of incomplete dissolvation of DNA pellets in 1M NaCl leading to abnormally low P atomic concentrations. The full sets of force-spacing curves and ion partition-spacing relations are provided in the Supplementary Information (Figs. S1 and S2).

Fig. 2. The partition of CoHex (f_{Co}) as a function of bath [Mg^{2+}] under constant osmotic pressures given by the legend in weight/weight [PEG8k]s. Symbols are the measured f_{Co} values and lines are the fits with the phenomenological model described by Equation 1. Separated panels are used here to avoid cluttering of the curves, and the results under additional osmotic pressures are shown in Suppl. Fig. S4.

Fig. 3. The force magnitudes of repulsion (Π_R, □) and attraction (Π_A, ○) from fitting the force-spacing curves with double exponentials described in Equation 1. (a) The magnitudes are shown as functions of the bath [Mg^{2+}]. (b) The magnitudes are shown as functions of the representative ion partition f_{Co} values at an intermediate DNA-DNA d-spacing ~26 Å.

Fig. 4. Comparison between experimental and predicted DNA-DNA spacings. The force-space relations $\Pi(d,f_{Co})$ under bath salts of CoHex only (f_{Co}=1) and Mg^{2+} only (f_{Co}=0) are used to predict the d-spacings under mixed bath salts as described in the main text. A total of 9 series are shown in respective symbols for the bath salts of CoHex 1 mM and Mg^{2+} 2 (□), 5(○), 7(▷), 10 (◊), 12 (Δ), 15 (◁), 17 (▽) and 20 (☆) mM. The dashed line gives the y=x curve.

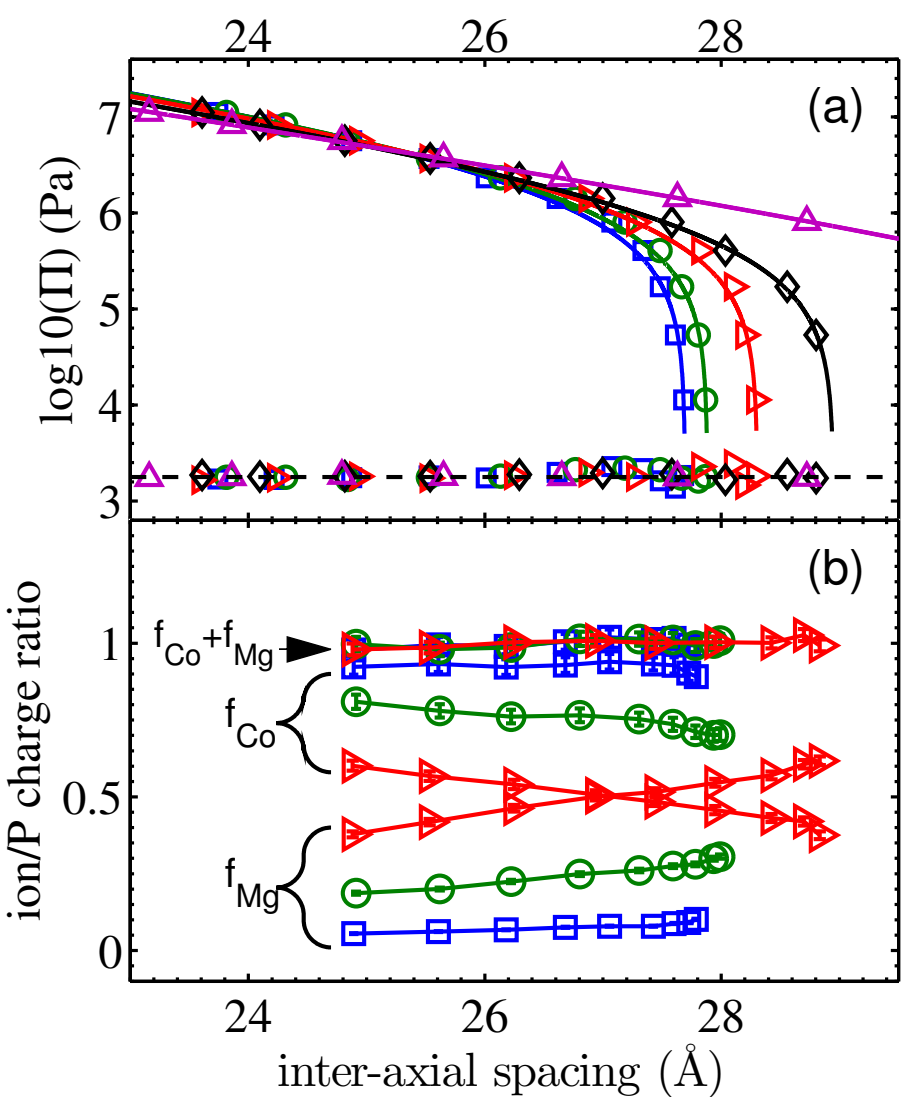
24
26
28
(a)
log10(Π) (Pa)
7
6
5
4
3
(b)
ion/P charge ratio
1
0.5
0
f_Co+f_Mg
f_Co
f_Mg
24
26
28
inter-axial spacing (Å)

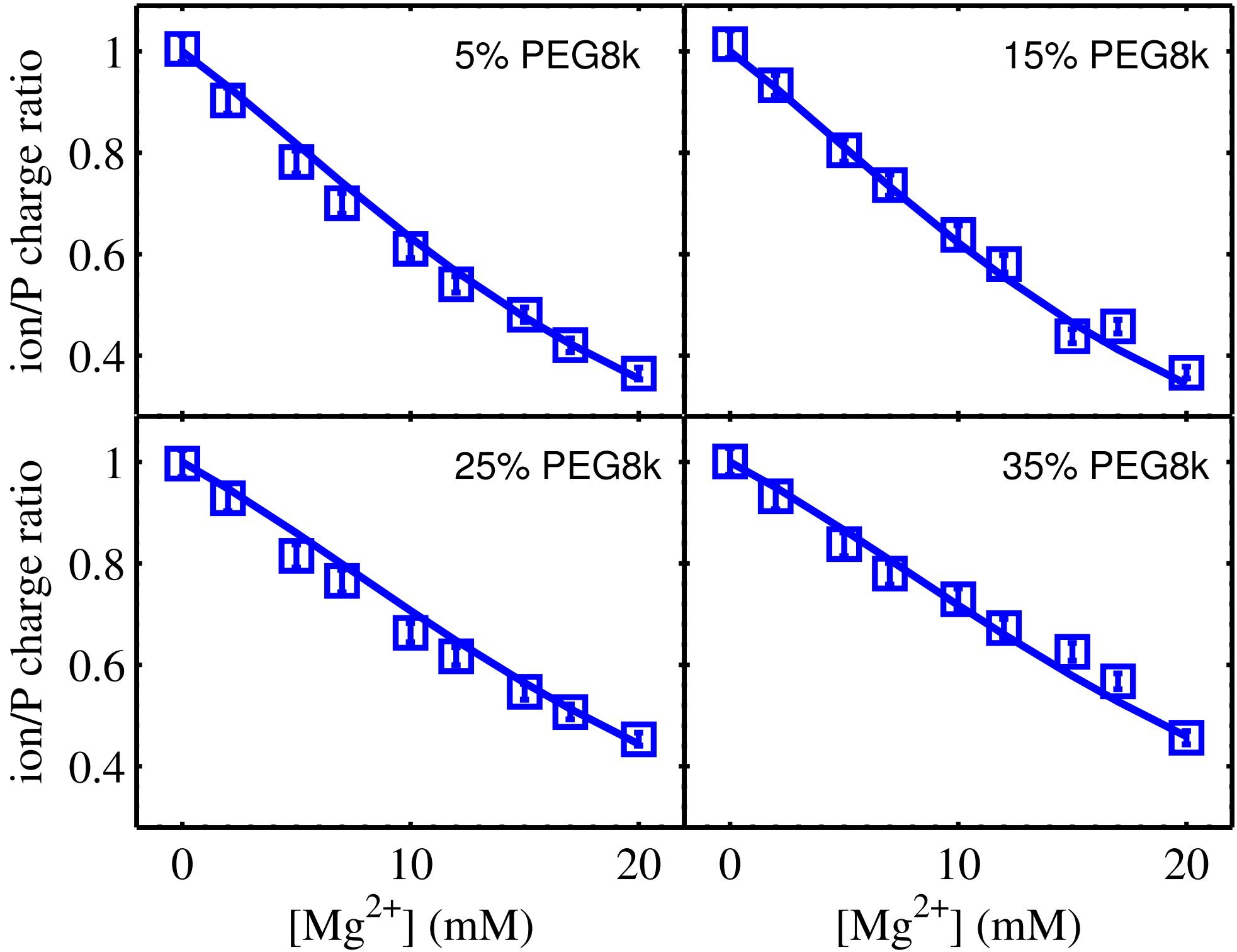
5% PEG8k
15% PEG8k
25% PEG8k
35% PEG8k
ion/P charge ratio
ion/P charge ratio
1
0.8
0.6
0.4
0
10
20
0
10
20
[Mg2+] (mM)
[Mg2+] (mM)

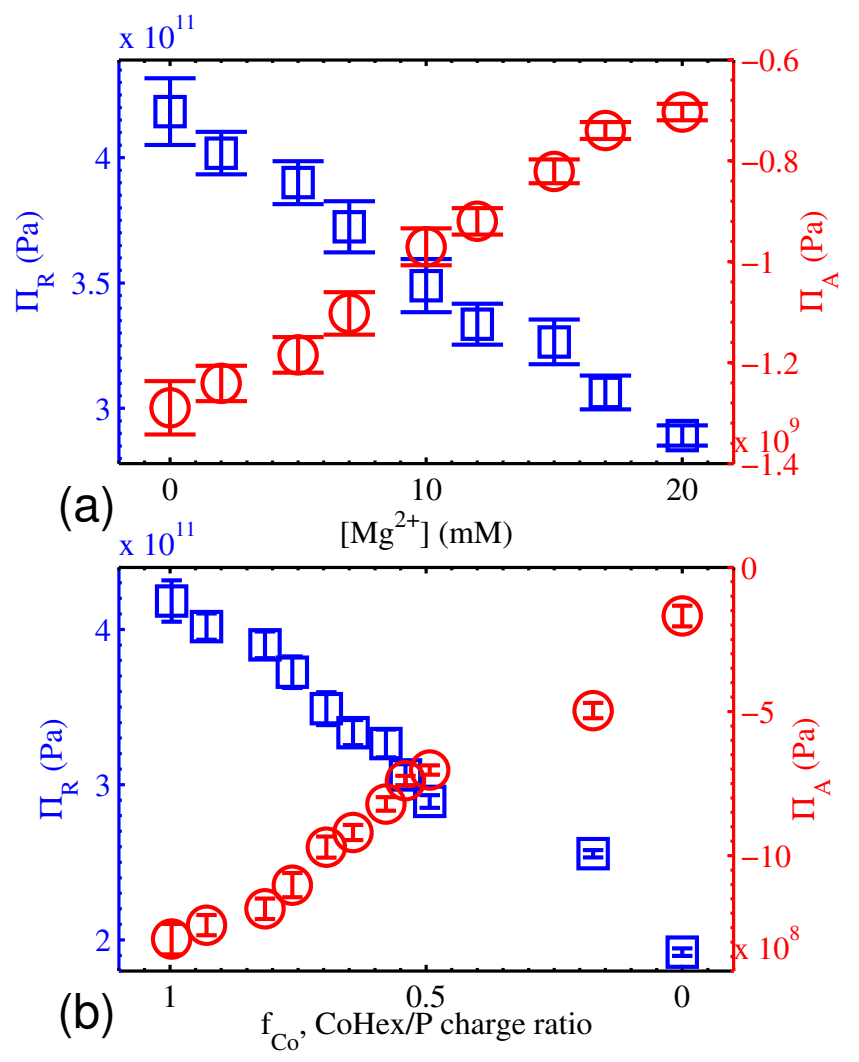
x 10^11
Π_R (Pa)
Π_A (Pa)
x 10^9
[Mg^2+] (mM)
(a)
x 10^11
Π_R (Pa)
Π_A (Pa)
x 10^8
f_Co, CoHex/P charge ratio
(b)

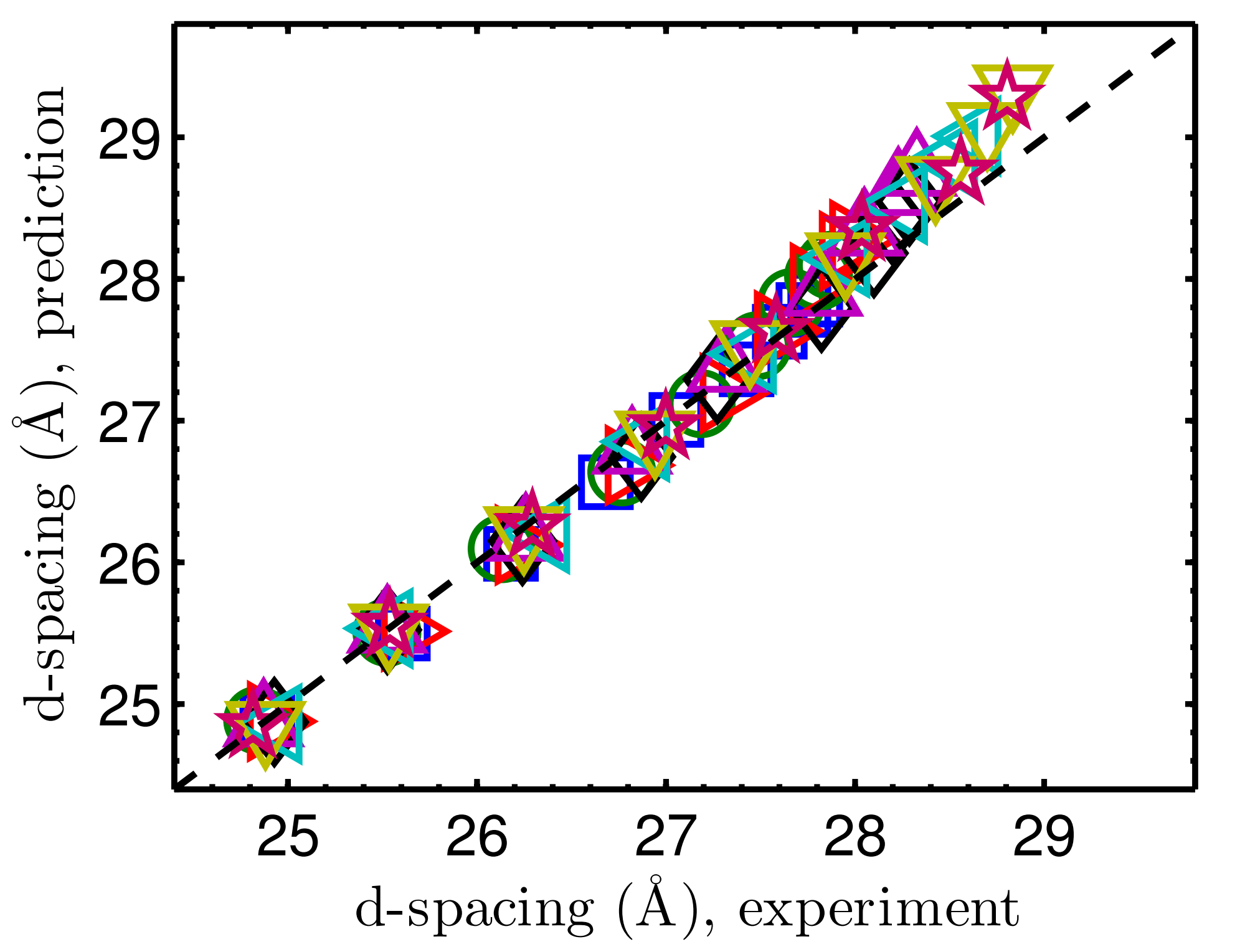
d-spacing (Å), prediction
25
26
27
28
29
d-spacing (Å), experiment
25
26
27
28
29